
CLOUD VOIDS - INTERPRETATION AND EXPLANATION

This chapter presents experimental, theoretical and numerical results concerning cloud voids. Cloud voids are a phenomenon that was registered only once and was published for the first time in **Karpinska2019** by the author of this thesis and others, including the experimental group. [1.1](#) presents the experimental results in details. [1.2](#) proposes the necessary conditions for cloud void formation, assuming the model exploited in ?? in polydisperse particle case. ??? dokonczyc po napisaniu rozdzialu

CLOUD VOIDS EXPERIMENT RESULTS

Cloud voids observations were performed at UFS on Zugspitze slopes in August 2011. Experimental methods used were described in Sec.?. This section presents the measurement results.

First, 30-minute long records of turbulence and droplet properties corresponding to the camera acquisition series in two measurement days were chosen for analysis. Droplet size raw measurements are presented in Fig. [1](#) and the corresponding statistics in Table [1](#). Both cloud droplets, as well as drizzle drops were captured. On August 29th the droplet number concentration was visibly larger. Unfortunately the device deficiency did not allow for reliable measurement of the droplet concentration on August 29th. Next, the probability distribution of the droplet size has been calculated and presented in Fig.[2](#). There are clear differences between the distributions measured on both days: the first one is much wider, the tail reach larger values and on average the droplets are about twice as big.

High-resolution measurements of small-scale turbulence during cloud void events were conducted. Applying the methods described in Sec. [??](#), mean energy dissipation rates and Kolmogorov scales were determined. Droplet and turbulence measured properties together with derived parameters are summarized in Table [1](#). Values of dimensionless parameters were calculated with the use of mean radius and Kolmogorov timescale. There is about one order of magnitude difference in St between two cases, but the Froude numbers are comparable.

Multiple cloud images and movies were collected by laser-sheet imaging technique on the measurement days. In general two kinds of events in which droplet spatial distribution is visibly inhomogeneous were distinguished. The first kind is characterized by an irregular interface separating clear-air and cloudy-air volumes and/or cloudy volumes of visibly different properties over a wide range of spatial scales (panel b) in Fig. [3](#)). Inhomogeneities of the second kind,

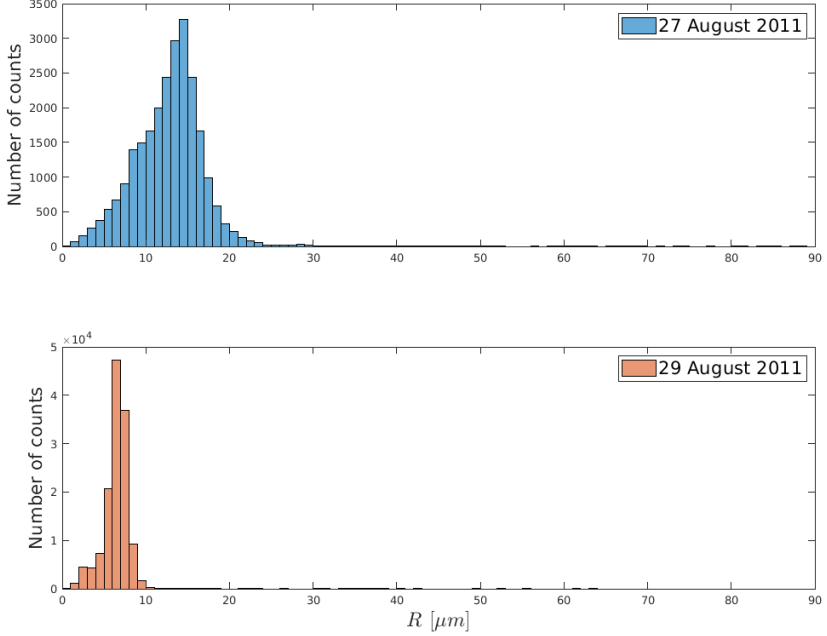


Figure 1: Histograms of droplet size counts measured with a PDI probe at the UFS on 27th and 29th of August 2011.

Table 1: Properties of turbulence and cloud droplets during 30-minutes long observation periods. Values of dimensionless parameters are calculated with the use of mean radius.

	August 27th	August 29th
Energy dissipation rate ϵ [cm ² /s ³]	550	700
Kolmogorov length scale η [mm]	0.50	0.47
Komogorov timescale τ_η [ms]	17	15
Droplet radius R [μm]	12.9 ± 4.8	6.4 ± 1.5
Stokes number St	0.126	0.035
Sedimentation parameter S _v	0.676	0.172
Froude number Fr	0.186	0.203
Number density n [cm ⁻³]	56 ± 47	no data

present within the cloudy volumes, were called cloud voids in "Swiss cheese" clouds. Cloud voids were small (a few centimetres scale), the interface was usually blurry (see panels a) and c) in Fig. 3) and the shapes of clear-air regions were often close to round or elliptic (see magnified voids in Fig. 4). It is important to point out that the more intuitive expression "cloud holes" with regards to the second kind inhomogeneities is avoided on purpose because it is commonly used referring to the cloud-free regions occurring in stratocumulus decks, as described for example in Gerber_2005.

Inhomogeneities of the first kind are argued to be created in the process of cloud – clear-air mixing (e.g. [Warhaft_2000]). In contrast, in some series of images and movies, the shape of the recorded tracks of cloud droplets suggest the following cloud void origin hypothesis: they result from interactions between inertial, heavy cloud droplets and small-scale vortices present in a turbulent cloud. Comparison of

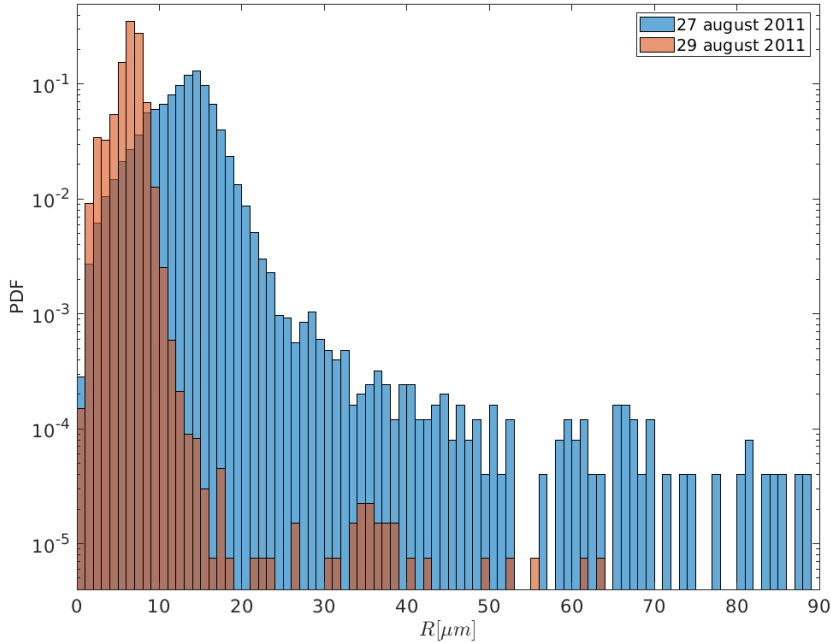


Figure 2: Droplet size probability distributions calculated for the data obtained with a PDI probe at the UFS on 27th and 29th of August 2011.

the two described cases becomes straightforward when conducted on the basis of the enclosed movies [**database**]. In the movie "ms01" between 13 s and 22 s there are two cloud void appearances. Motion of the void in the homogeneous cloud field resembles motion of a worm. Movie "ms02" presents cloudy and clear air mixing at the cloud edges.

There were a few series of cloud void images collected with various laser-camera settings on the two experimental days. The best quality series, made in the morning of the 27th, was chosen for void size analysis. For the series of 17 photos selected for analysis, there were four in which voids were not clear enough to be accounted for. In the remaining 13 photos 27 voids were identified. Each one's size was manually determined. In the case of a round void, the diameter was taken as the size; in a case of flattened or ellipsoidal void, the maximal chord was taken. The typical void diameter was estimated to be 3.5 ± 1 cm; the maximal, 12 ± 4 cm; the minimal, 1 ± 0.5 cm. Images from the analysed series from the morning of August 27th showing examples of objects identified as voids are presented in the panel a) of Fig. 3. Voids captured on the 29th of August were not analysed due to the large uncertainty resulting from the unknown geometry of the camera-laser set-up. The general experimental observation was that the voids were smaller than those on August 27th. Definitive experimental verification of the cloud void origin is not possible on the basis of collected data only; however, in next sections, I argue that void creation due to inertia of droplets present inside vortex tubes is highly probable.

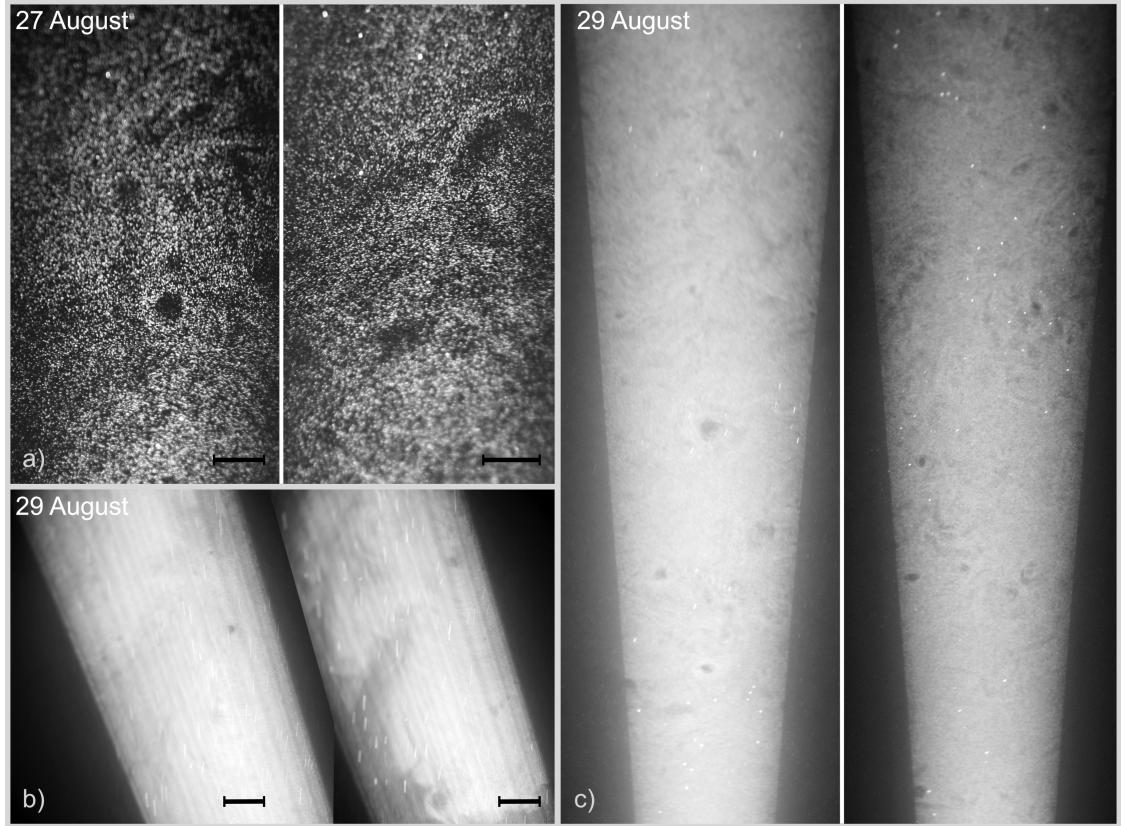


Figure 3: Examples of cloud voids observed at the UFS station with various camera-laser configurations. Images taken on 27 August (panel a) were chosen to estimate cloud void sizes. The ones recorded on 29 August evening (panel b) show the difference between inhomogeneities produced by cloud voids and those resulting from the mixing with clear air at the cloud edge. Other images from 29 August (panel c) suggest that the voids can be quite frequent in the sample volume. Bright spots and lines are due to presence of larger precipitation particles. 10 cm long segment is shown to represent spatial scale assumed in the void size calculation. For more details, see the movies attached in the supplementary materials.

CLOUD VOID CREATION CONDITIONS

Lets assume that cloud voids are caused by the presence of a long-lasting vortex that appear numerously in turbulence structure and lets use the model of particle motion in a vortex explored in ??, applied to cloud particles in atmospheric turbulence. Is the model able to produce a "void effect"? If yes, what are the necessary conditions? How they translate to model parameters? This section tries to answer all these questions.

The use of analytical model requires the precise definition of a void. For the start, we have a collection of cloud droplets of certain size distribution, distributed uniformly in the air, where the appearance of a Burgers vortex of a certain size, circulation and gravity alignment, creates a void of a few centimetres size, lasting a few seconds. Here the void is defined as an inhomogeneity in droplet field, a region almost devoid of droplets. It has nearly cylindrical shape, in the cross section it takes a form close to a circle or an ellipsoid. In order to obtain a void using the model, the following hypothesis on polydisperse particle collective behaviour are formulated. Firstly, the major

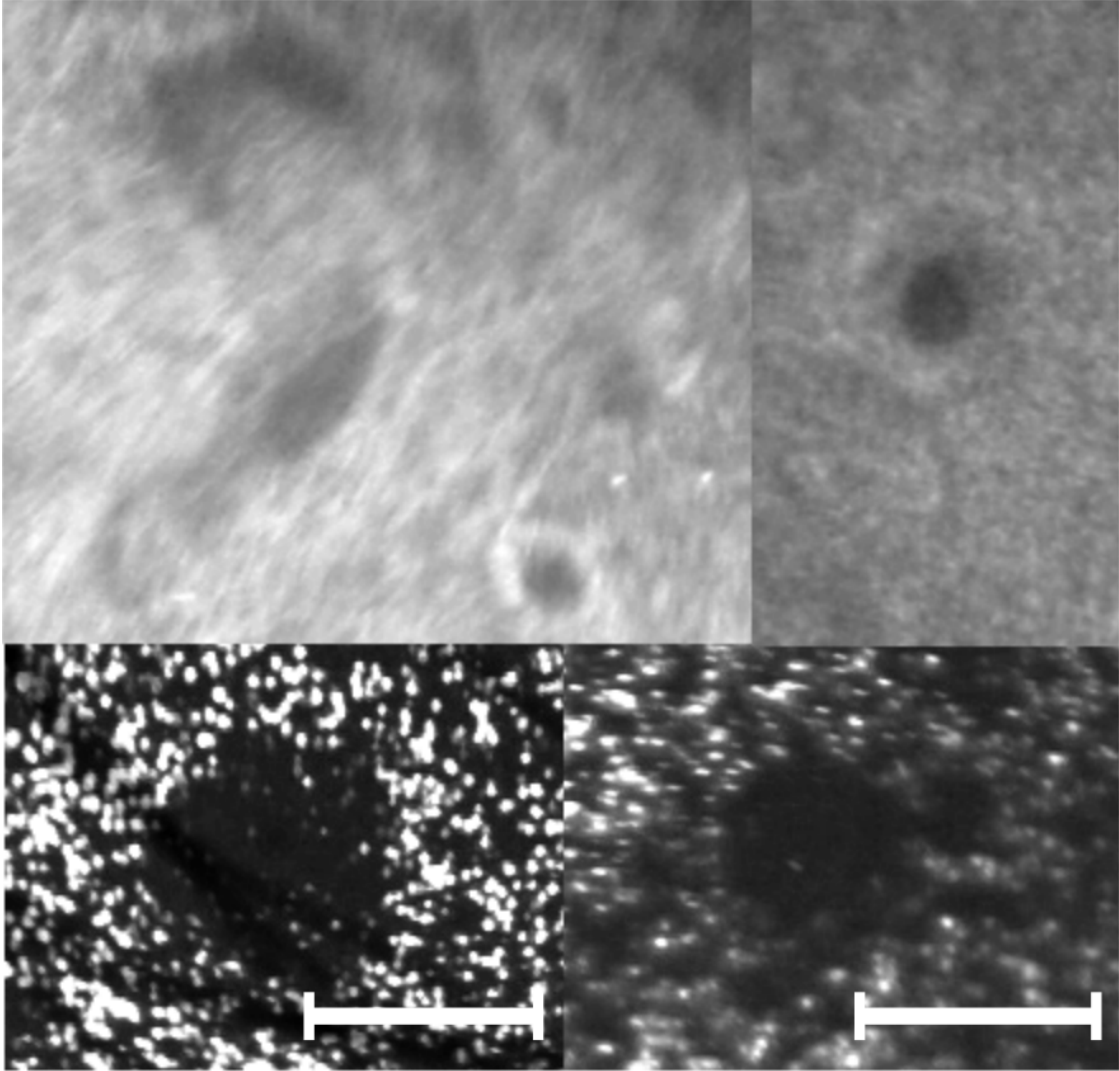


Figure 4: Example close-ups of variously shaped cloud voids observed at the UFS station with different camera-laser configurations. 5 cm long section is placed in each image to represent spatial scale assumed in the void size calculation.

ity of droplets' trajectories are determined by limit cycle attraction. Secondly, the radius of curvature of the limit cycle is large enough to recognize it, as the void in observations is clearly distinguishable from random spatial distribution fluctuations. Attraction by a single stable equilibrium point far from the axis is not considerable, so the trajectories do not cross the void. Finally, the time needed to form the void is shorter than exit time for most of the particles. These conditions are inspected in the following subsections.

Polydisperse particles motion analysis

The conditions defined above for the motion of the polydisperse collection of droplets in the 2D space are met if most of the drops realize motion scenarios referred to in Fig. ?? as (1b)-(3b), and possibly only a small part of the largest droplets of scenario (5). If there is a void characterized by (A, δ, θ) , then the size range $[R_<, R_>]$ of particles that realize one or more of the scenarios (1b)-(3b) is constrained. All of the particles must have at least one unstable focus r_0^+ near the axis. This

is guaranteed by the two conditions: $r_0^+ < r_s$ and $A < A_{\max}(R, \delta, \theta)$ for all $R \in [R_<, R_>]$. So for a vortex described by (A, δ, θ) the range $[R_1, R_2]$ is approximately defined by A_{\max} as described in last paragraph of ???. However, it can be further restricted by the condition $r_0^+ < r_s$. To verify the last, a value called R_s is calculated numerically and it is defined by the relation $r_0^+(R_s, A, \delta, \theta) = r_s$. Finally, limit cycle is a solution for a range of particle radii $[R_<, R_>]$ if:

- $R_1 < R_s < R_2$, then $R_< = R_1, R_> = R_s$, or
- $R_1 < R_2 < R_s$, then $R_< = R_1, R_> = R_2$.

Figure 5 presents results of numerical calculations of R_1, R_2, R_s in the vortex parameters domain, specific for cloud-like conditions (first, second and third row respectively). Color scale was selected to be common to all three variables. Alignment angle θ cases are arbitrary, but smaller than $\pi/4$, for the clarity of the figures. For the larger the angle, the narrower the A and δ domain in which limit cycle is a solution. The fourth row shows the difference $R_2 - R_s$. R_1 decreases when strain parameter A decreases (circulation increases) or vortex size δ decreases. On the contrary to R_1, R_2 and R_s increase when strain parameter A decreases (circulation increases) or vortex size δ decreases. The last row reveals, that the inequality sign between R_2 and R_s is not constant, but changes with vortex parameters. $R_>$ should be calculated in two ways, depending on these parameters.

Figure 5 shows final results: left margin of the range $R_>$, right margin of the range $R_<$ and their interval magnitude, at the same time giving approximate parameter ranges of cloud void-creating vortex. Values presented in the figure reach from well below 1 to around 25 μm , so they are relevant for cloud droplets.

- There is a threshold (minimal) value of circulation needed for void creation. It increases with inclination angle ($\sin \theta$) and vortex size δ .
- The greater the circulation the smaller particles have their unstable points near the axis.
- The range of particles having unstable points near the axis increases with increasing circulation and decreases with increasing gravity influence and vortex size δ .

Building up on these results it may be concluded that it is harder to observe voids created by horizontally aligned vortices than vertically aligned ones and also more difficult to observe voids the larger particle size range is.

Particle orbit in a void - the radius of curvature

In order to obtain a void, a majority of the droplets must circle around the axis and the curvature of their trajectories should be large enough for a void to be noticeable. In order to estimate the curvature radius we perform the following reasoning. Firstly, a basic vortex spatial scale is established for the measurement conditions. Premises found

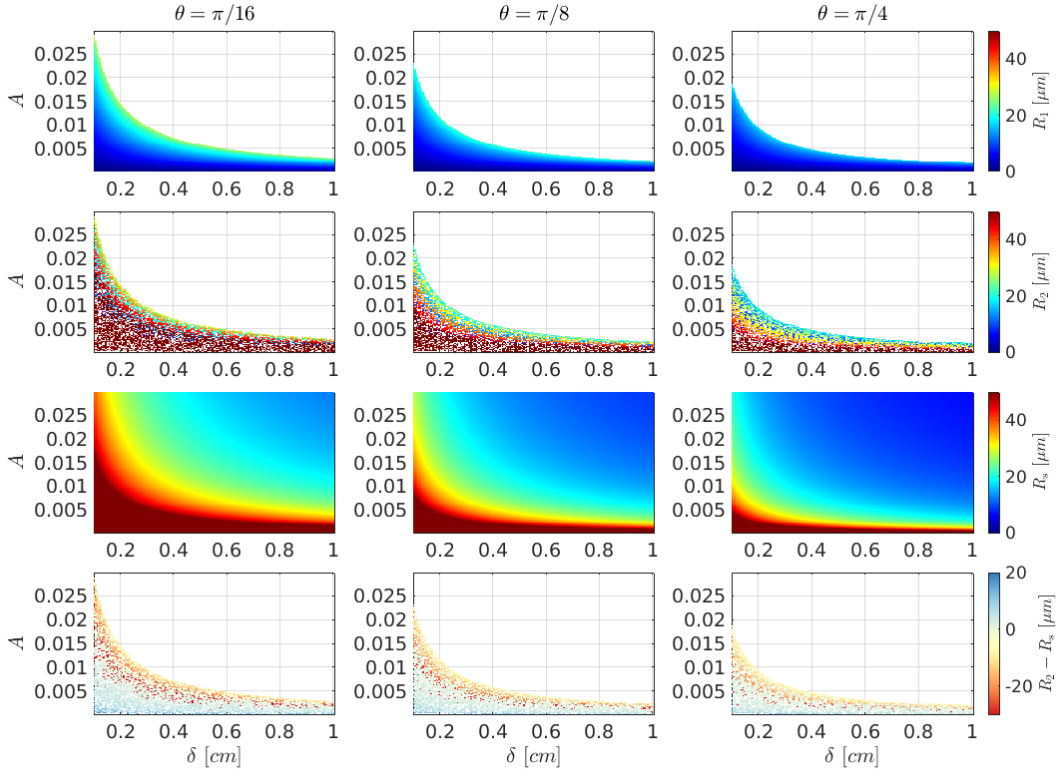


Figure 5: Approximated size range of particles $[R_1, R_2]$ that has a limit cycle solution, represented by color scale, with respect to vortex parameters (first and second row), R_s (third row), as defined in the text body and the interval between R_2 and R_s (fourth row), obtained numerically. Colorscale is common for R_1 , R_2 and R_s , separate for $R_2 - R_s$. Three alignment angle values selected are represented in columns. Vortex parameters domain corresponds to cloud-like conditions.

in the literature discussed in the introduction were used for making the assumption that the proportionality constant in Eq. ?? is in the range $m \in [3.5, 24]$. It means $\delta \in [0.18, 1.20]$ cm for August 27th measurements. Secondly, the droplet trajectory curvature radius is approximated by the periodic orbit radius which is a solution of Eq. ???. For this reason, solutions of Eq.?? are presented in Fig.?? for various representative vortex parameters. Every color represents one of droplet sizes: $R = 3, 13, 23 \mu\text{m}$ chosen to be within the experimental range for August 27th (see Table ??). Overlapping colored surfaces match regions in which solutions can exist (what corresponds to the condition $St < St_{cr}$). Dashed lines are contour plots of solutions of chosen (close to experimental) void sizes: 0.5 cm, 1.5 cm, 3 cm. Using the information presented in this plot, the analysed strain parameter was further limited, from $A < A_{cr}$ down to $A \in [10^{-4}, 8 \cdot 10^{-3}]$.

Figure 7 shows the results of r_{orb} calculation in a different view. It illustrates the contour plots for selected orbit radii (0.5 cm, 1.5 cm, 3 cm). Overlapping (blue on a top, then pink and green) coloured surfaces match subspaces of stable periodic orbit existence.

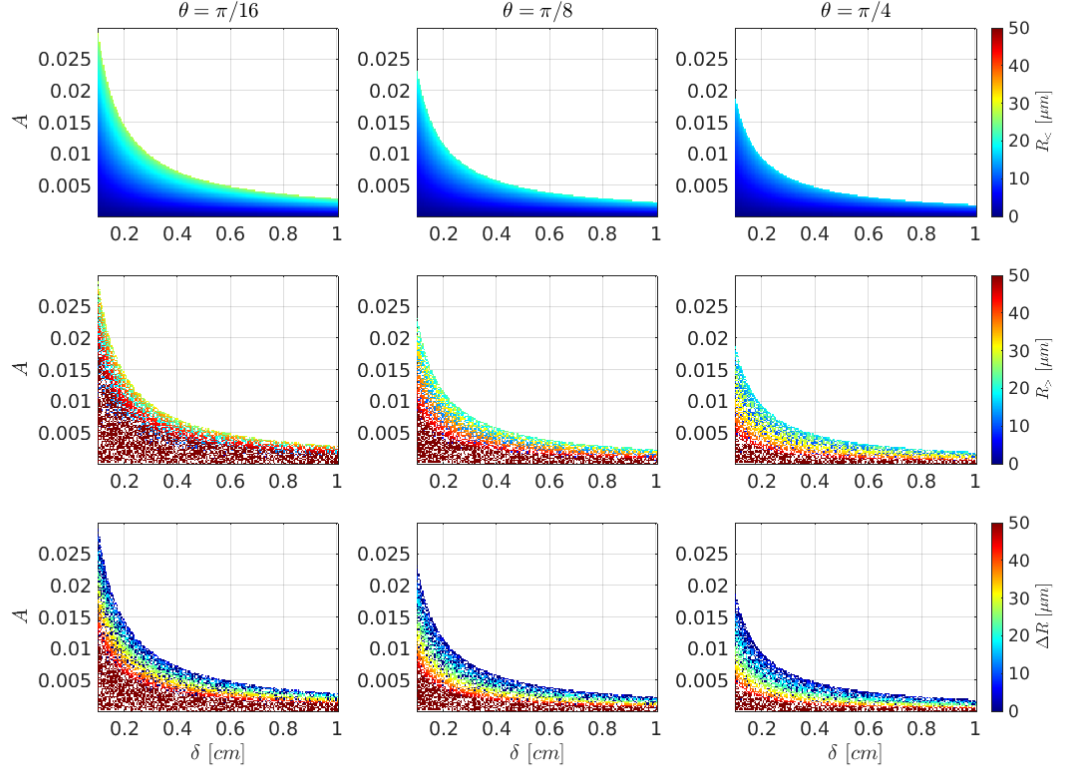


Figure 6: Numerical calculation of approximated size range of particles $[R_<, R_>]$ (first and second row) that create a cloud void, as well as interval between them ΔR (third row) in relation with vortex parameters. Colorscale is common for all the variables. Three alignment angle values selected are represented in columns. Vortex parameters domain corresponds to cloud-like conditions.

Timescales of motion

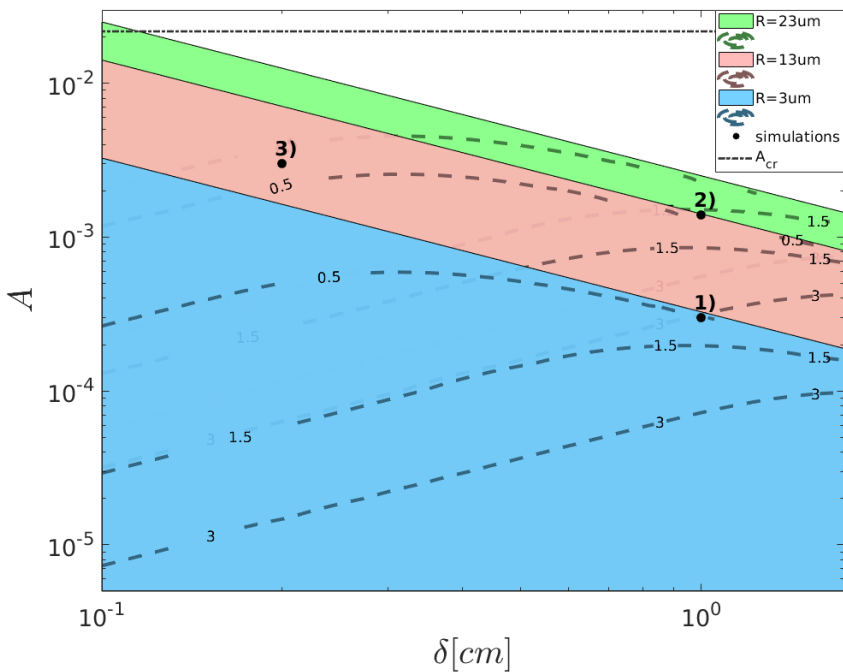


Figure 7: Contour plot of stable periodic orbit radius for droplets of radii $R = 3, 13, 23 \mu\text{m}$ for cloud-like parameter ranges of δ and A . Overlapping (blue on a top, then pink and green) colored surfaces match subspaces in which stable periodic 2D orbit exist for droplet radius given by its colour. Dashed lines are contour plots for r_{orb} equal to 0.5 cm , 1.5 cm , 3 cm . Black points represent simulation parameters sets (refered to in ???).